CORE
Metadata, citation and similar papers at core.ac.uk
Provided by Explore Bristol Research

Silvestri, M., Uren, M. J., & Kuball, M. (2013). Iron-induced deep-level acceptor center in GaN/AlGaN high electron mobility transistors: Energy level and cross section. Applied Physics Letters, 102(7), 073501. 10.1063/1.4793196

Link to published version (if available):
10.1063/1.4793196

Link to publication record in Explore Bristol Research
PDF-document

University of Bristol - Explore Bristol Research

General rights

This document is made available in accordance with publisher policies. Please cite only the published version using the reference above. Full terms of use are available: http://www.bristol.ac.uk/pure/about/ebr-terms.html

Take down policy

Explore Bristol Research is a digital archive and the intention is that deposited content should not be removed. However, if you believe that this version of the work breaches copyright law please contact open-access@bristol.ac.uk and include the following information in your message:

• Your contact details
• Bibliographic details for the item, including a URL
• An outline of the nature of the complaint

On receipt of your message the Open Access Team will immediately investigate your claim, make an initial judgement of the validity of the claim and, where appropriate, withdraw the item in question from public view.

Iron-induced deep-level acceptor center in GaN/AlGaN high electron mobility transistors: Energy level and cross section

Marco Silvestri[a)], Michael J. Uren, and Martin Kuball

Center for Device Thermography and Reliability (CDTR), H.H. Wills Physics Laboratory, University of Bristol, BS8 1TL, Bristol, UK

Dynamic transconductance dispersion measurements coupled with device physics simulations were used to study the deep level acceptor center in iron-doped AlGaN/GaN high electron mobility transistors (HEMTs). From the extracted frequency dependent trap-conductance, an energy level 0.7eV below the conduction band and a capture cross section of 10^{-13} cm^2 were obtained. The approach presented in this work avoids the non-equilibrium electrical or optical techniques that have been used to date and extracts the device relevant trap characteristics in short channel AlGaN/GaN HEMTs. Quantitative prediction of the trap induced transconductance dispersion in HEMTs is demonstrated.

Keywords: AlGaN/GaN HEMT, iron doping, deep level center, transconductance dispersion.

[a)] Electronic mail: Marco.Silvestri@bristol.ac.uk

GaN-based high electron mobility transistors (HEMT) deliver highly promising performance in high-power switching, RF, and microwave applications. To achieve such performance short channel effects are commonly controlled via the introduction of deep level acceptors[1]. The introduction of Fe or C, for example, prevents punch-through, buffer leakage current and provides insulation and carrier confinement[2,3]. However, the beneficial effect of such intentional doping can be deleterious in terms of electrical performance in some circumstances causing an increase in on-resistance under transient conditions, or a DC-RF dispersion (or current-collapse) in microwave devices limiting the available current and output power[4,5,6,7]. Despite the fact that Fe is now widely used during growth of GaN buffer layers for HEMTs, knowledge about its detailed trap characteristics is surprisingly still sparse. So far, only non-equilibrium electrical and optical techniques on GaN layers have been used to study this trap center, reporting energy levels for the Fe^{2+}/Fe^{3+} in the range between 0.28 eV and 1 eV below the GaN conduction band[8,9,10]. However, the trap level which is normally important for transistor operation is that which is determined under equilibrium conditions. A common approach for the determination of trap response time is the conductance technique[11] or related approaches[12]. These normally rely on capacitance measurements, but cannot be straightforwardly used either in short channel HEMT devices due to the small capacitance or in large area devices due to the lateral channel resistance[13].

In this work we take advantage of the dynamic transconductance dispersion technique[14] that has been recently proven to be a powerful tool to extract trap details in AlGaN/GaN HEMTs in quasi-equilibrium conditions[15,16]. In particular, Fe trap characteristics are determined using short-channel devices for a range of buffer Fe doping concentrations.

<u>Fe-doped AlGaN/GaN HEMTs with 4µm source-drain gap, 0.25-µm channel length, and silicon nitride passivation were studied. The epitaxial layer structure was grown by metal-</u>

organic vapor phase epitaxy and had a 26-nm $Al_{0.22}Ga_{0.78}N$ barrier, a 1.9 µm GaN layer, and an AlN nucleation layer on a semi-insulating 4H-SiC substrate. Intentional iron doping was implemented during GaN growth by a surface segregation mechanism[17] with three residual channel concentrations, namely ~$7x10^{15}$ cm^{-3}, ~$3.6x10^{16}$ cm^{-3}, and ~$1.5x10^{17}$ cm^{-3}, denoted in the following as low-, medium- and high-Fe, respectively. Fig. 1 shows a secondary ion mass spectroscopy (SIMS) analysis for the three different wafers. The iron density is constant in the bulk and then decreases exponentially towards the surface, once the Fe doping is switched off during growth at depths between 0.5 µm and 1.1 µm. Carbon contamination during growth was measured by SIMS for similar wafers to those used for device fabrication and was found to be below the background of a few times 10^{16} cm^{-3}, as can be seen in Fig. 1.

For the dynamic transconductance measurement, the devices were operated in the sub-threshold region to avoid the influence of the inversion layer capacitance and in the ohmic regime, with a drain bias of 50 mV, to probe the whole gated channel area. The drain current was measured with a low noise current to voltage converter and the dynamic transconductance dispersion measurements have been performed with a frequency response analyzer in the range 1 Hz – 10 kHz and with different base plate temperatures.

The dynamic transconductance dispersion technique probes traps below the gated region of the device relying on a direct correlation between the inverse of the imaginary part of the transconductance and the trap conductance through $G_p/\omega=-I_d q C_b (kT)^{-1} Im(1/g_m)$ where I_d is the drain current, q is the elementary charge, C_b is the AlGaN barrier capacitance, k the Boltzmann constant, and T the temperature in Kelvin and the device is operated below pinch-off[13,14]. The resulting trap conductance amounts to a measurement of the dispersion or loss in the transconductance, with observed phase angles of up to a few degrees and a system resolution of better than 10^{-1} degree. The technique is sensitive to traps within a few kT/q around the Fermi level, avoiding unwanted trapping phenomena and associated transient

effects during measurement. Discrimination between buffer and interface traps is also possible by studying the bias dependence of the conductance. As opposed to buffer traps that do not show any bias dependence, interface states would show a strong variation of the electron concentration with bias and hence would show a resulting change in response frequency[11]. The ability of this technique to discriminate between such traps avoids misleading interpretations associated with false trap-related signatures from different locations in the device[18]. More details on the technique can be found in Ref. 14.

Simulations were performed with the Silvaco ATLAS code considering an AlGaN/GaN HEMT with the same dimensions as the measured devices. The net charge at the AlGaN surface was set to zero corresponding to full compensation of the surface polarization charge by surface donor states, and the polarization charge at the AlGaN/GaN interface and GaN mobility were adjusted to give reasonable agreement with the DC transconductance and pinch-off voltage. Self-heating and impact ionization were not implemented, which is justified due to the low currents and low fields applied during the measurements, as was gate tunneling, excluding all surface or gate related effects. Shockley-Read-Hall and Fermi-Dirac statistics were enabled. The buffer Fe doping profile was varied according to Fig. 1, and as in reference 4, 10^{15} cm^{-3} shallow compensating donors were included in all cases representing the effect of background contamination by species such as Si.

Figure 2 illustrates the trap conductance G_p/ω for a representative high Fe-doped device for different baseplate temperatures. The G_p/ω exhibits a loss peak around 10 Hz at 293 K. From the shift of the G_p/ω peak with temperature an activation energy, E_A, of ~0.7 eV was determined, (inset of Fig. 2). The capture cross section was estimated at room temperature to be ~$4x10^{-13}cm^2$ through the relation $\sigma=1/(N_b v_t \tau)$ where $N_b=N_c exp(-E_A/kT)$ is the carrier concentration in the bulk with N_c the density of states in the GaN conduction band, $v_t=2x10^7$ $cm \cdot s^{-1}$ is the thermal velocity, and assuming a uniform energy distribution of traps the

characteristic time $\tau=1.98/(2\pi f_{peak})$ with f_{peak} the G_p/ω peak frequency value[11]. As shown in Fig. 2 the conductance peak shape agrees well with the commonly used Lehovec theoretical model representing the conductance G_p/ω for a continuum of trap energy levels where the trap areal density and the time constant have been varied to achieve the fit[11].

Measurements were performed for AlGaN/GaN HEMTs with different buffer Fe concentrations, and are reported in Fig. 3. In the case of the high Fe concentration (Fig. 3a) the trap conductance was almost one order of magnitude higher than the lowest Fe density considered (Fig. 3c). The correlation with the iron doping concentration and the fact that no gate bias dependence to the peak frequency was observed implies that these are iron-related buffer traps rather than interface states. The trap activation energies extracted from the temperature sweeps of the three wafers were found to be all consistent and around 0.7 eV. This is within the range of 0.28 eV – 1 eV reported in the literature, however performed here on application relevant devices in a quasi-static way.

Figure 3 illustrates the result of the ATLAS device simulation. A small-signal AC simulation was performed and the imaginary part of the transconductance was extracted from the transistor Y-parameters. Simulations captured the behavior of the measured dispersion using as input the iron doping profiles shown in Fig. 1, a common Fe energy level, 0.72 eV below the conduction band that leads to an activation energy of 0.7 eV, and capture cross-section that best fits the conductance peak frequency as summarized in Table I. No further fitting parameters were used.

TABLE I. Extracted activation energies and capture cross sections of Fig. 3 at 293K

	Low Fe		**Medium Fe**		**High Fe**	
	Data	Sim.	Data	Sim.	Data	Sim.
Activation energy [eV]	0.72	0.7	0.66	0.7	0.68	0.7
Capture cross section [cm^2]	8×10^{-13}	5×10^{-14}	1×10^{-13}	8×10^{-14}	4×10^{-13}	1×10^{-13}

Good agreement was achieved for all the devices considered in this work. In particular the simulation accurately predicted the magnitude of the dispersion confirming the physical mechanism at the root of the phenomenon and the trap modeling technique. All the simulations were performed under the assumption of fully active iron doping and given the excellent agreement to the data we can infer that the iron in and near the device channel is mostly active in contrast to reference 19 where a compensation ratio of 34% was found.

The measurement probes the Fe doping concentration where the Fermi level crosses the iron level in the buffer. Figure 4 shows the simulated GaN conduction band and the iron acceptor trap level of 0.72 eV below the conduction band for the three iron concentrations as a function of the depth below the AlGaN layer. This figure is plotted for a common drain current of 10^{-6} A and at 293 K to enable easy comparison. The Fermi level crosses the Fe level at different bias dependent depths: the low, medium, and high Fe concentration sampled at depths of 200 nm, 95 nm, and 55 nm, respectively. The measured variation in dispersion magnitude seen in Fig. 3 is fully consistent with this doping concentration variation.

Simulations were also carried out using an active carbon concentration of 10^{16} cm^{-3} in line with Fig. 1 and no shallow compensating donors, so that the Fermi level was pinned deep in the bulk of the GaN near the C level which is reported to be 0.9 eV above the valence band[20]. This still resulted in a very similar Fe-trap response. The reason why the Fe related response appears to be broadly unaffected by low densities of these other impurities is that the Fermi level must always cross the Fe trap level in the bulk of the GaN and thus will always respond to the AC excitation.

The Fe acceptor in GaN is reported as having a wide variety of energy levels, however the measurements are consistent with the conclusion that the Fermi level is tied to the Fe^{2+}/Fe^{3+} transition located 0.72eV below the conduction band. The large capture cross-section of 10^{-13} cm^2 is suggestive of a Coulomb attractive center and again is consistent with this attribution[21].

This trap characterization for GaN has allowed a device physics based simulation to be undertaken and a key transistor property to be quantitatively predicted: the small-signal transconductance dispersion. This understanding of the GaN buffer will give increased confidence in the ability to design and specify future GaN transistors.

Acknowledgments

We would like to thank the UK Engineering and Physical Science Research Council (EPSRC), for supporting this work under the grant EP/I033165/1, and QinetiQ Ltd and the UK Ministry of Defence for providing the devices.

References

[1] M. J. Uren, K. J. Nash, R. S. Balmer, T. Martin, E. Morvan, N. Caillas, S. L. Delage, D. Ducatteau, B. Grimbert, and J. C. De Jaeger, *IEEE Trans. Electron Dev.,* vol. 53, pp. 395-398, 2006.

[2] S. Heikman, S. Keller, S. P. DenBaars, and U. K. Mishra, *Applied Physics Letters,* vol. 81, p. 439, 2002.

[3] C. Poblenz, P. Waltereit, S. Rajan, S. Heikman, U. K. Mishra, and J. S. Speck, *J. Vac. Sci. Technol*. B22 (3), 1145 (2004).

[4] K. Horio and A. Nakajima, *Japanese Journal of Applied Physics*, vol. 47, pp. 3428-3433, May 2008.

[5] M. J. Uren, J. Möreke, and M. Kuball, *IEEE Trans. Electron Dev.*, vol. 59, no. 12, pp.3327-3333, 2012.

[6] S. C. Binari, P. B. Klein, and T. E. Kazior, *Proc. of the IEEE*, vol. 90, no. 6, June 2002.

[7] E. Bahat-Treidel, F. Brunner, O. Hilt, E. Cho, J. Wurfl, and G. Trankle, *IEEE Trans. Electron Dev.,* vol. 57, pp. 3050-3058, Nov 2010.

[8] R. Heitz, P. Maxim, L. Eckey, P. Thurian, A. Hoffmann, I. Broser, K. Pressel, and B. K. Meyer, *Phys. Rev*. B 55 (7), 4382 (1997).

[9] T. Aggerstam, A. Pinos, S. Marcinkevicius, M. Linnarsson, and S. Lourdudoss, *J. Electronic Mater.* 36 (12), 1621 (2007).

[10] A. Y. Polyakov, N. B. Smirnov, A. V. Govorkov, A. A. Shlensky, K. McGuire, E. Harley, L. E. McNeil, R. Khanna, S. J. Pearton, and J. M. Zavada, *Phys. Stat. Sol. (c),* vol. 2, pp. 2476-2479, 2005.

[11] H. Nicollian and J. R. Brews, *MOS physics and technology,* Wiley, New York, 1982.

[12] D. K. Schroder, *Semiconductor Material and Device Characterization*, Third Edition, John Wiley & Sons, Inc., Hoboken, NJ, USA, 2006.

[13] H. Haddara, T. Elewa, and S. Cristoloveanu, *IEEE Electr. Dev. Lett.,* vol. 9, no. 1, pp. 35-37, January 1988.

[14] H. Haddara and G. Ghibaudo, *Solid-State Electronics*, vol. 31, no. 6, pp. 1077-1082, 1988.

[15] W. Kruppa, S. C. Binari, and K. Doverspike, *Electronics Letters*, vol. 31, no. 22, pp. 1951-1952, 26th October 1995.

[16] M. Silvestri, M. J. Uren, and M. Kuball, *IEEE Electron Dev. Lett*., vol. 33, no.11, pp. 1550-1552, 2012.

[17] R. S. Balmer, D. E. J. Soley, A. J. Simons, J. D. Mace, L. Koker, P. O. Jackson, D. J. Wallis, M. J. Uren, and T. Martin, *Phys. Stat. Sol. (c),* vol. 3, pp. 1429-1434, 2006.

[18] G. Verzellesi, M. Faqir, A. Chini, F. Fantini, G. Meneghesso, E. Zanoni, F. Danesin, F. Zanon, F. Rampazzo, F.A. Marino, A. Cavallini, A. Castaldini, *47th Annual IEEE International Reliability Physics Symposium,* pp. 732-735, 2009.

[19] S. Heikman, S. Keller, T. Mates, S. P. DenBaars, and U.K. Mishra, *J. Crystal Growth* 248, 513 (2003).

[20] J. L. Lyons, A. Janotti, and C. G. Van de Walle, *Applied Physics Letters,* vol. 97, p. 152108, 2010.

[21] J Bourgoin and M Lannoo, *Point Defects in Semiconductors II.* (Springer-Verlag, 1983).

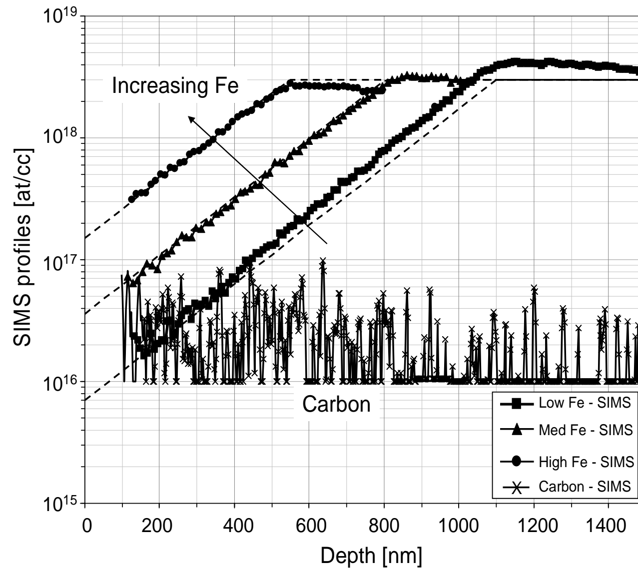

Figure 1: GaN buffer iron density profiles of the investigated AlGaN/GaN devices from SIMS analysis. The dashed lines show the profiles used in the simulation. The carbon profile measured in a similar wafer is also shown.

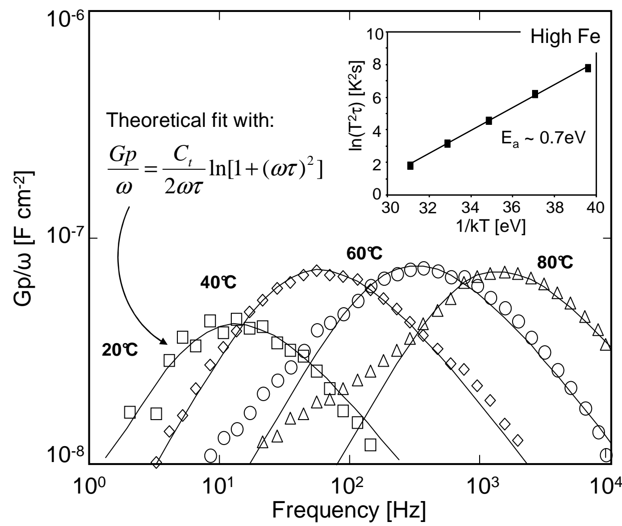

Figure 2: Trap conductance as a function of frequency for different baseplate temperatures for a representative high Fe-density AlGaN/GaN HEMT. The inset displays the activation energy extraction.

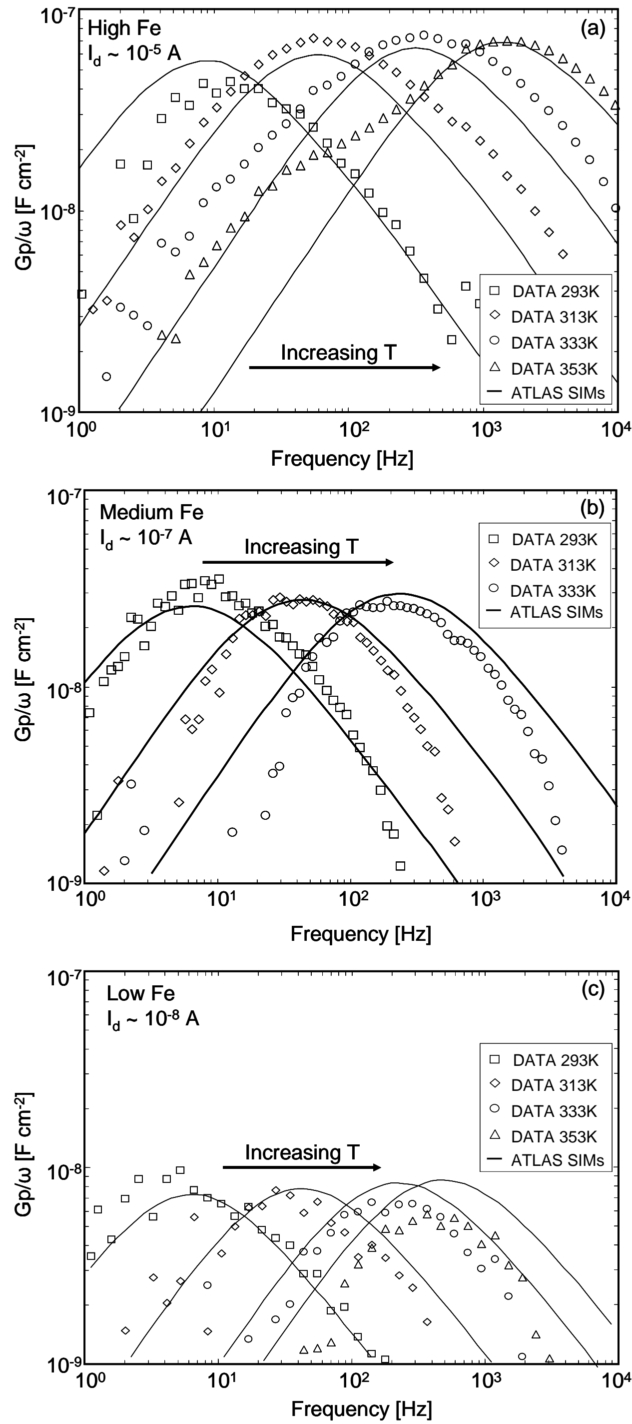

Figure 3: Measured (symbols) and simulated (solid lines) trap conductance as a function of frequency for different baseplate temperatures for (a) high, (b) medium, and (c) low residual GaN channel iron doping concentration.

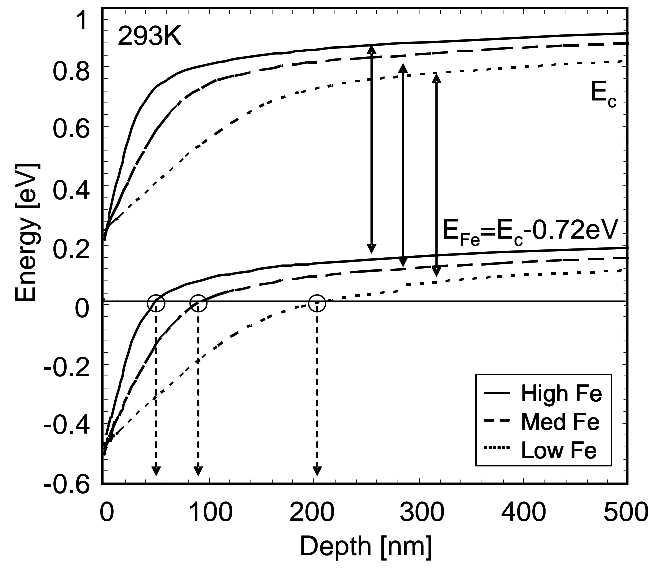

Figure 4: Simulated GaN conduction band diagram for the three iron doping concentrations at room temperature for a drain current around 10^{-6} A. The iron level E_{Fe} is located 0.72 eV below the conduction band.